

# Wavelet Filtering of Speckle Noise - Some Numerical Results

Langis Gagnon  
Centre de Recherche Informatique de Montreal,  
550 Sherbrooke Ouest, Montreal QC, Canada, H3A 1B9  
langis.gagnon@crim.ca

March 7, 1999

## Abstract

*We present our most recent results about an ongoing study addressing the comparison of various speckle reduction filters. In a previous work, we have concentrated on the best Signal-to-Mean-Square-Error (S/MSE) ratio provided by a complex Wavelet Coefficient Shrinkage (WCS) filter and several standard speckle filters. Here we specifically address the numerical behavior of the WCS filter over a change (1) in the regularity and type of the wavelet (orthogonal versus bi-orthogonal) and (2) in the wavelet coefficient thresholding type (soft- versus hard-thresholding). We also present measures of the variation of the S/MSE over a wide range of the WCS filter parameters in order to provide information on the optimal application range of the filter in practical situations. As in our previous work, tests are performed on optical imagery with a simulated multiplicative Log-Normal noise. The S/MSE ratio is measured after averaging the filtered images over 16 diagonal shifts of the Discrete Wavelet Transform (DWT) in order to approximate a shift invariant DWT. Our experiments show, among other, that the optimal threshold level depends on the spectral content of the image and that the soft-thresholding scheme is the best choice for images with high spectral content.*

## 1 Introduction

The aim of this paper is to present recent results about an ongoing study addressing the comparison of various speckle reduction filters. In previous works [1, 2], we have concentrated on the best Signal-to-Mean-Square-Error (S/MSE) ratio provided by a complex Wavelet Coefficient Shrinkage (WCS) filter and several standard speckle filters that are widely used in the radar imaging community (Lee, Kuan, Frost, Geometric, AFS, Gamma and Oddy). It has resulted that the complex WCS filter was among the best ones, quantitatively and qualitatively. In particular, the filter was clearly outperforming the standard ones for images with large speckle noise; up to 10% improvement on a low

spectral content image.

In the current work, we specifically address the numerical behavior of the WCS filter over a change (1) in the regularity and type of the wavelet (orthogonal versus bi-orthogonal) and (2) in the wavelet coefficient thresholding type (soft- versus hard-thresholding). In addition, we found very much instructive to measure the variation of S/MSE over a wide range of the complex WCS filter parameters, because it provides much information on the optimal application of the filter in practical situations.

The paper is organized as follows. In the next subsections, we provide some background about speckle statistics and the measure we use to quantify the filtering process. In Section 2, we describe the filters we are comparing in this report. Section 3 presents a comparative results, in tables and graphics form, for 2 standard filters and the WCS filter with various wavelets (complex orthogonal and bi-orthogonal) and thresholding procedures. A brief wrap-up is given in Section 4.

### 1.1 Speckle

Speckle noise is a common phenomena in all coherent imaging systems like laser, acoustic and SAR imagery. The source of this noise is attributed to random interference between the coherent returns.

Fully developed speckle has the characteristics of a random multiplicative noise. Theoretically, under the assumption that the real and imaginary parts of the speckle signal have zero-mean Gaussian density, speckle intensity can be shown to follow a Gamma distribution [3]. Experimental speckle distributions can deviate from the theoretical Gamma distribution. For instance, Log-Normal distribution satisfying

$$X_{Log-Normal} = m \exp \left( X_{Normal} \sqrt{2 \log(M/m)} \right)$$

where  $M$  and  $m$  are the mean and median values and

$X_{Normal} \sim N(0, 1)$ , turns out to be a good speckle model for high-resolution sea-clutter imagery [4]. Because our comparative study originates from ocean surveillance applications, we are still retaining this distribution here.

## 1.2 Quantitative Measure

Let  $x$  be an image pixel corrupted by a stationary multiplicative noise  $n$  such that  $y = nx$ . Without loss of generality, we assume noise of unit-mean ( $\bar{n} = 1$ ). Many standard filters require knowledge of  $\bar{y}$ ,  $\sigma_y$  and  $\sigma_n$ . In practice,  $\bar{y}$  and  $\sigma_y$  are estimated locally, within a finite size window. Noise standard deviation  $\sigma_n$  is given as an input filter parameter (or estimated over a uniform area in the image).

A common way of estimating the speckle noise level in coherent imaging is to calculate the mean-to-standard-deviation ratio of the pixel intensity, often termed the Equivalent Number of Looks (ENL), over a uniform image area. Unfortunately, we found this measure not very robust mainly because of the difficulty to identify a uniform area in a real image. For this reason, we will only use here the S/MSE ratio, defined as,

$$S/MSE = 10 \log \left( \frac{\sum x_i^2}{\sum (y_i - x_i)^2} \right)$$

and which corresponds to the standard SNR in case of additive noise. The filters retained in this study are described in the following.

## 2 Speckle Filters

Standard speckle filters are the Median, Lee, Kuan, Frost, Gamma and Geometric filters. They usually perform efficiently on most images (especially Frost and Gamma). Wavelet-based filters are essentially based on a WCS approach that aims at obtaining an optimal trade-off between good signal averaging over homogeneous regions and minimal resolution degradation of image details. We have recently proposed such a filter, based on the Symmetric Daubechies (SD) wavelets [1, 2].

### 2.1 Frost Filter

The Frost filter [5] is an adaptive Wiener filter which involves the pixel values within a fixed size window with an exponential impulse response  $m$  given by

$$m = \exp[-KC_y(t_0)||t||] \quad C_y = \sigma_y/\bar{y}$$

where  $K$  is the filter parameter,  $t_0$  represents the location of the processed pixel and  $||t||$  is the distance measured from pixel  $t_0$ . This response results from an autoregressive exponential model assumed for the scene reflectivity  $x$ .

### 2.2 Gamma Filter

The Gamma filter is a Maximum A Posteriori (MAP) filter based on a Bayesian analysis of the image statistics [6]. It assumes that both the corrupted signal and the speckle noise follow a Gamma distribution. The ‘‘superposition’’ of these distributions yields a K-distribution which is recognized to match a large variety of radar return distributions of land and ocean targets. The estimate  $\hat{x}$  is given by

$$\hat{x} = \frac{(\alpha - L - 1)\bar{y} + \sqrt{\bar{y}^2 (\alpha - L - 1)^2 + 4\alpha L y \bar{y}}}{2\alpha}$$

$$\alpha = \frac{L + 1}{L (\sigma_y/\bar{y})^2 - 1}$$

where  $L$  is the number of looks. We have put  $\hat{x} = \bar{y}$  for the pathological cases where  $\hat{x}$  is negative or complex.

### 2.3 Wavelet Filter

Details about the theoretical foundation of DWT can be found in numerous places. Here we will give a brief summary in terms of linear algebra and for a 1D signal. One can extend the description to images, similarly than Fourier transform, i.e. by processing rows and columns sequentially.

A one-level DWT of a vector  $\vec{x} = (x_1, \dots, x_N)$  (representing the  $N$  samplings of a 1D signal) is represented by a (generally complex)  $N \times N$  block-circulant matrix  $W$ . The vector  $\vec{w}$  of wavelet coefficients is then simply given by  $\vec{w} = W \vec{x}$ . The inverse transform is represented by a matrix  $\widetilde{W}$  such that  $\widetilde{W}W = I$ . If the transform is orthogonal, then  $\widetilde{W} = W^T$ , otherwise the DWT is said to be bi-orthogonal. The fundamental block of  $W$  is a  $2 \times L$  matrix  $B$  ( $L < N$ ) where one row operates as a low-pass filter while the second is a high-pass filter. The elements of  $B$  depends on the (bi-)orthogonality and regularity conditions imposed to the wavelet basis. Half of the elements of  $\vec{w}$  encodes the local details of  $\vec{x}$  (the so-called wavelet coefficients) while the other half encodes the local tendencies. A multi-level DWT is computed via a pyramid algorithm where a half smaller matrix  $W$  operates on the ‘‘tendency’’ outputs of the previous level.

### 2.3.1 Wavelet Coefficient Shrinkage

Most of the wavelet speckle filters are based on the WCS procedure for discrete wavelet transform [7]. Wavelet coefficients of a function are, in general, large in irregular regions and small in uniform regions. If the function is corrupted by a noise, this noise will dominate the wavelet coefficients at finer scales and only few large coefficients will be related to the strong singularity of the underlying function. Thus, thresholding the noisy wavelet coefficients removes most of the noise and preserves large coefficients. The two more popular thresholding schemes are the so-called soft- and hard-thresholding. In both cases, the threshold level  $T$  is proportional to the noise standard deviation  $S$ . Hard-thresholding consists in putting to zero all wavelet coefficients of amplitude smaller than  $T$ . Soft-thresholding additionally reduces the amplitude of the other coefficients by the quantity  $T$ . In practice, for Gaussian additive noise,  $S$  is estimated by the standard deviation of the wavelet coefficient distribution at the finest scale, and  $T = \delta S$ , where  $\delta$  is a free denoising parameter. For multiplicative noise, it is usual to take the logarithm of the signal prior the wavelet transform.

The WCS procedure applies similarly on images, by considering independent noise estimate and thresholding in each of the 3 spectral bands (the so-called HH, HV and VH blocks).

### 2.3.2 Symmetric Daubechies (SD) Wavelets

The WCS procedure is mathematically optimal for orthogonal wavelet transform (real or complex Daubechies' wavelets). Use of complex Daubechies' wavelets however requires slight modification in the procedure in order to manage the complex-valued characteristic. We have proposed the following one [1, 2]. We have numerically observed that complex wavelet coefficients generally follow a bi-Normal distribution (Figure 1a). Since the "spatial" properties of this distribution is a characteristic of the image, it seems natural to modify the WCS procedure in order to perform thresholding that preserves the distribution eccentricity and the principal axes orientation. As a result, the threshold level becomes angle-dependent and extends in proportion to the eccentricity of the centered dispersion ellipse. Figure 1b,c shows the effect of a hard- and soft-thresholding rule, respectively, on the distribution of Figure 1a. Since the threshold curve is completely set by the distribution eccentricity, one can take  $\delta$  as the threshold proportionality factor along the first principal axis. In addition, the complex wavelet distributions are generally oriented differently in each block, and for each level, for a 2D signal (image).

In our previous reports, we have restricted the comparison of the wavelet-based speckle filter to standard ones, us-

ing 6-tap (i.e.  $L = 2J + 2$  with  $J = 2$ ) SD wavelets together with a soft-thresholding scheme [1, 2]. It was shown that the SD wavelet-based filter outperforms the standard ones, especially for high-level noise. Here we want to investigate more deeply the effect of changing the filter regularity and the thresholding scheme. The selected wavelets is the J2 wavelet as well as the representative of the J4, J6 and J8 classes having the highest maximum value in the low-pass filter [8]. The corresponding scaling functions allow exact representations of polynomials of order 2, 4, 6 and 8 respectively.

### 2.3.3 Bi-orthogonal Wavelets

Another important set of wavelets are the spline-based Cohen-Daubechies-Feauveau (CDF) bi-orthogonal wavelets. These are considered by many authors as the "wavelets of choice" for all kind of applications because of their unique properties (e.g. real and symmetric with odd support, possible integer scale implementation, etc.). The above WCS procedure is not optimal for bi-orthogonal wavelets. It has to be modified in order to incorporate correlations between nonorthogonal wavelet coefficients. A solution to this problem has been proposed recently [9]. The result consists in a modification of the  $\delta$  parameter which becomes wavelet- and scale-dependent. We are currently implementing this algorithm and the comparative results will be reported soon. In the mean time, we found instructive to test the robustness of a couple of bi-orthogonal filters against the orthogonal WCS approach. The selected CDF sets are the bi22, bi24, bi42 and bi44 wavelets for which the support of the low-pass and high-pass filters are (5,3), (9,3), (7,5) and (11,5), respectively. The synthesis low-pass filters of bi22 and bi24 are the B-spline of degree 1 while the synthesis low-pass filters of bi42 and bi44 are the B-spline of degree 3.

### 2.3.4 Shift Invariance

One disadvantage of the classical decimated DWT is its lack of shift invariance. As a result, wavelet decomposition of a signal differs when the signal is shifted by one data point. Of course, this can modify the noise estimate in the WCS procedure. One way to eliminate this drawback is to avoid decimation during the DWT [10]. Of course, not all shifts are necessary: for a  $N$ -level decomposition, only  $2^N$  shifts are needed. In doing so, one can show that the inverse transform is the average over all shifts of the decimated DWT [11].

As in our previous work, the S/MSE ratios we will be reporting are the average of the WCS filter over shifts of the input image. In practice, we found sufficient to restrict to 16

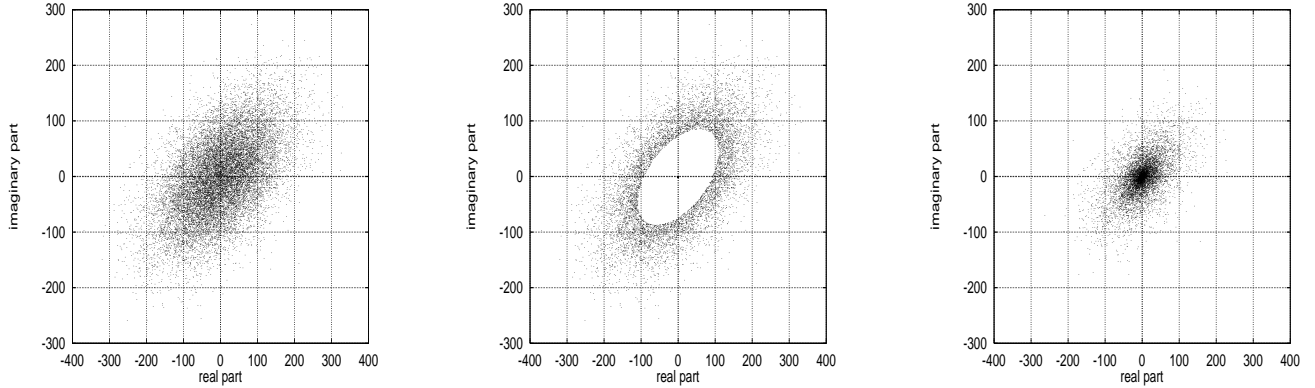


Figure 1: Illustration of elliptical thresholding rules on a complex wavelet distribution.

diagonal shifts (theoretically,  $2^N \times 2^N$  shifts should be used).

### 3 Tests

We have simulated radar textured images by degrading two aerial photographs ([www.cent.org](http://www.cent.org)) with unit-mean Log-Normal multiplicative noise. The two scenes (urban and country regions) have very different spectral content in order to observe their effect on the filters performance. Two noise levels have been tested, corresponding to S/MSE ratios of 4.4 and 9.8 dB. Figure 2 shows the original urban and country images as well as the corresponding 4.4 dB noisy images.

#### 3.1 Best S/MSE

The best quantitative performance measures for the Frost, Gamma and WCS filters are summarized in Table 1. Image radiometry (image intensity) has been preserved by assuring that the enhanced and noisy images have the same global mean. The best S/MSE is provided by the complex wavelet filter with a soft-thresholding scheme. The two best enhanced images (bold in Table 1) are depicted on Figure 3.

In all cases, the WCS filter outperforms the standard ones, and especially for the low spectral content image (country image) with high level noise (4.4 dB). Soft-thresholding scheme turns out to always give slightly better S/MSE than hard-thresholding, with a lower threshold level  $\delta$ .

#### 3.2 Numerical Behavior of the Wavelet Filter

As mentioned in the Introduction, we report here about the numerical behavior of the WCS filter over a change (1) in

the regularity and type of the wavelet (orthogonal versus bi-orthogonal), (2) in the wavelet coefficient thresholding type (soft- versus hard thresholding) and (3) in the variation of the filter parameters. This provides much information on the optimal application range of the filter in practical situations

Figure 4 first shows the variation of the S/MSE ratio for a soft-thresholding scheme for the urban scene for 4 decomposition levels, as function of the threshold parameter  $\delta$  and for different wavelet types. The best result is obtained with the complex J2 wavelet although there is not much difference with J4, J6 and J8 wavelets. Surprisingly, the bi-orthogonal b22 and bi24 wavelets perform quite well although the WCS algorithm is not optimal for them. The bi42 and bi44 wavelet are definitively not in the game. One also observes in Figure 4 that there is an optimal value for  $\delta$  above which the S/MSE starts decreasing because of the oversmoothing of the image.

The position of the optimal S/MSE depends on the wavelet (Figure 4) and on the number of decomposition levels (Figures 5 and 6). Of all the wavelets used in the tests, J2 provides the best performances. Furthermore, there is no advantage in using higher-order wavelets (J4, J6 and J8); they perform slightly less than J2 with a longer processing time. Surprisingly, bi22 and bi24 perform quite well too, given that the WCS scheme is not optimal for bi-orthogonal wavelets.

The wavelet thresholding scheme might limit the filter performance. Figure 7 shows the variation of the S/MSE ratio as function of  $\delta$ , for the urban and country scenes, using soft- and hard-thresholding with the J2 wavelet. This is especially true for the urban image which has a high frequency content. In addition, Figure 7 shows that the experimental optimal threshold level depends on the frequency content of the image. The enhanced images corresponding to the best S/MSE with a hard-thresholding are depicted in the bottom part of Figure 7.

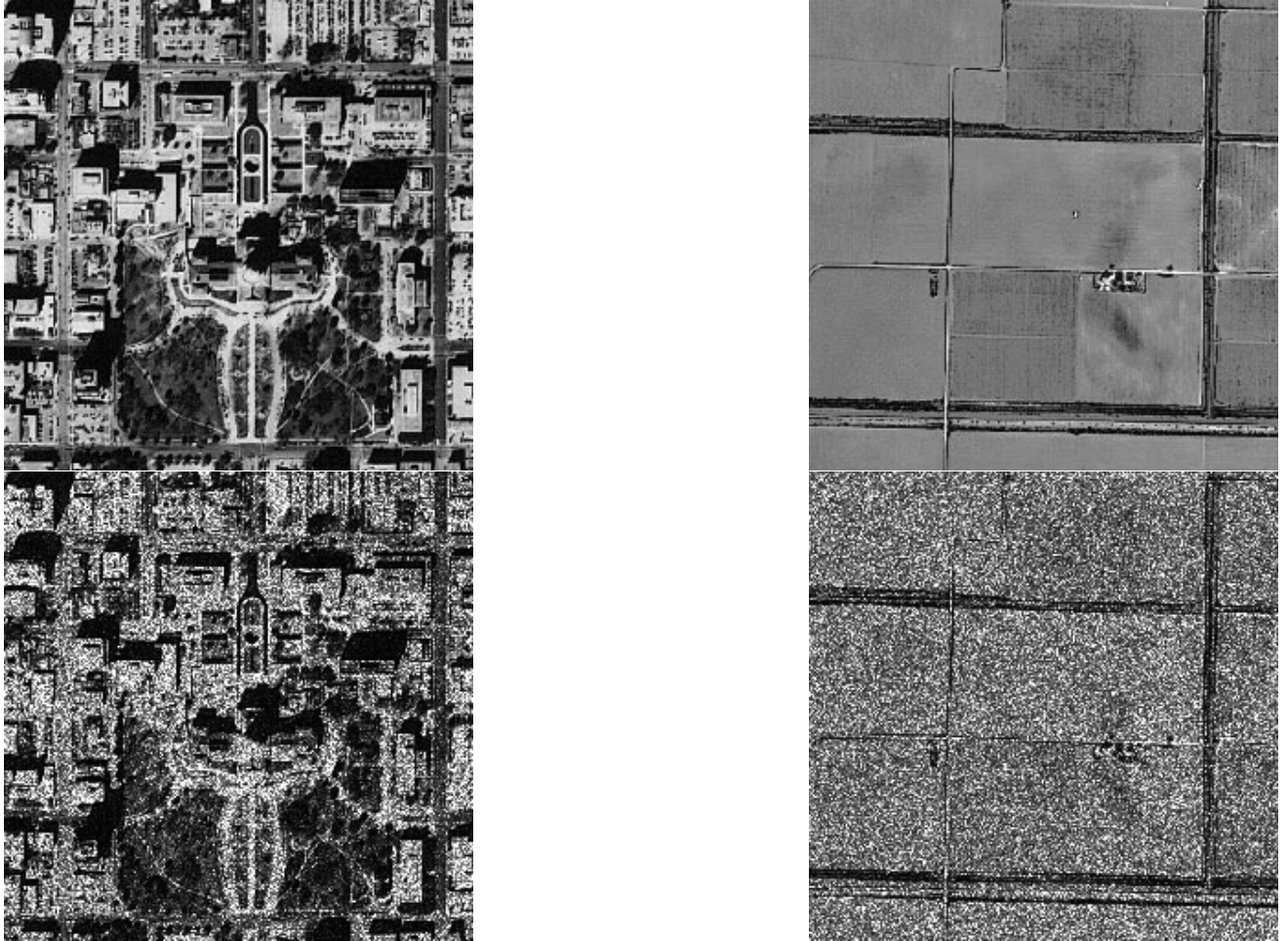


Figure 2: Test images: original (up) and noisy @ 4.4 dB (bottom)

	Frost	Gamma	Soft-with J2	Hard- with J2
Urban @ 4.4 dB	10.0 dB, $K = 1.0, 3 \times 3$	9.8 dB, $L = 1.5, 3 \times 3$	<b>10.9 dB</b> , $\delta = 1.4$	10.0 dB, $\delta = 2.8$
Urban @ 9.8 dB	13.4 dB, $K = 3.0, 3 \times 3$	13.3 dB, $L = 7, 3 \times 3$	13.6 dB, $\delta = 0.8$	12.4 dB, $\delta = 1.8$
Country @ 4.4 dB	14.6 dB, $K = 1.0, 7 \times 7$	14.5 dB, $L = 2.0, 7 \times 7$	<b>16.3 dB</b> , $\delta = 2.0$	16.0 dB, $\delta = 3.4$
Country @ 9.8 dB	17.4 dB, $K = 3.0, 7 \times 7$	17.7 dB, $L = 8, 7 \times 7$	18.6 dB, $\delta = 1.6$	18.5 dB, $\delta = 2.9$

Table 1: Best S/MSE obtained during the tests

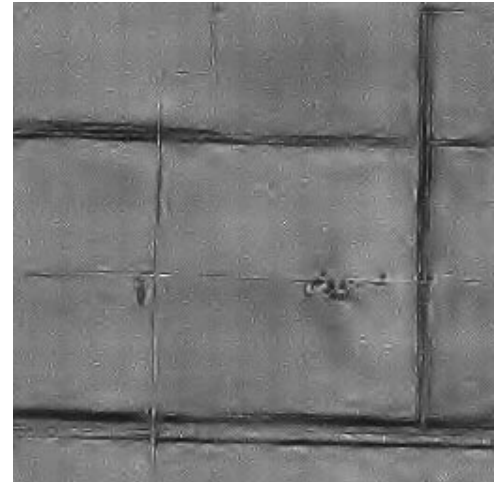


Figure 3: The two best enhancements @ 4.4 dB in Table 1 (bold)

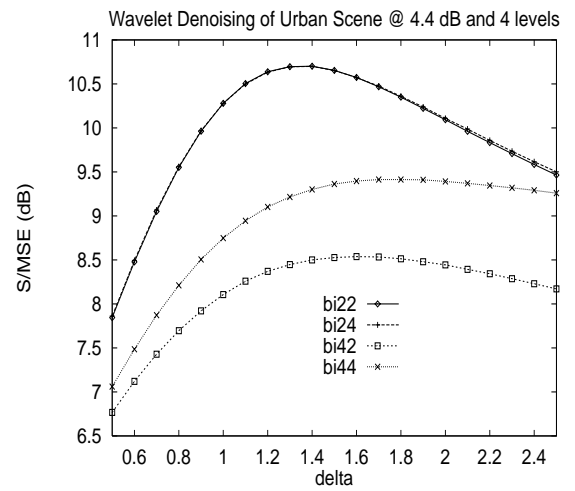
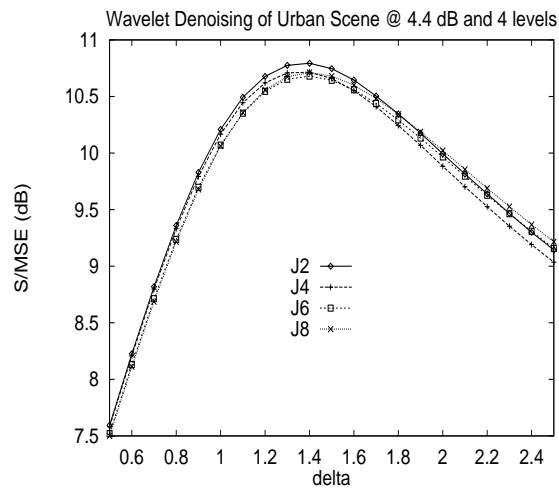


Figure 4: Wavelet denoising of the urban scene @ 4.4 dB and 4 levels

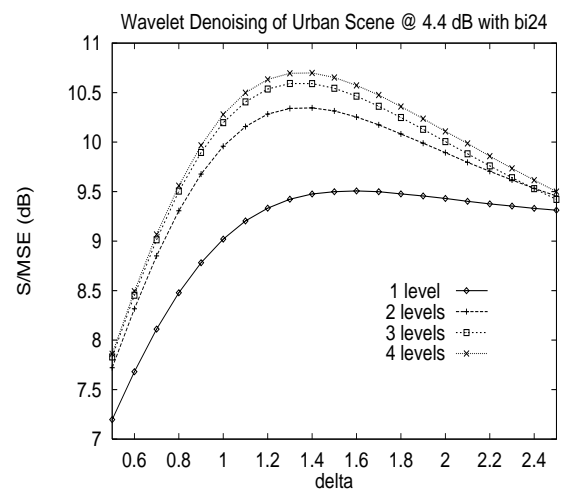
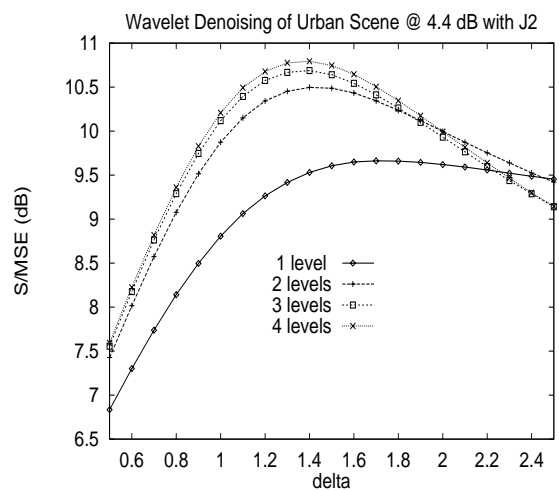


Figure 5: Wavelet denoising of the urban scene @ 4.4 dB with J2

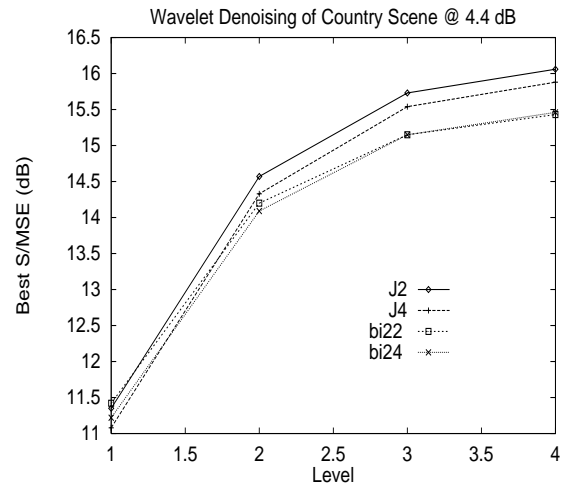
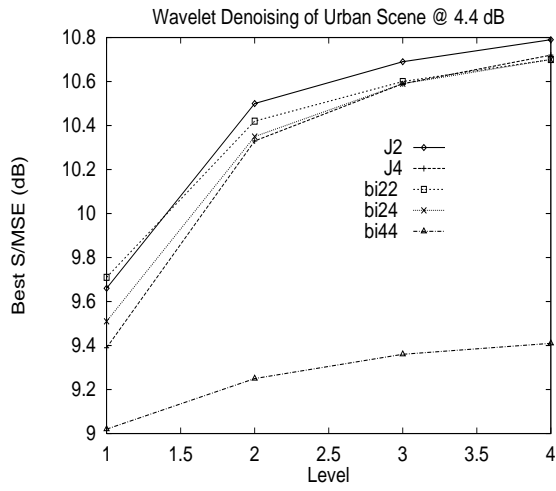


Figure 6: Wavelet denoising of the urban and country scenes @ 4.4 dB

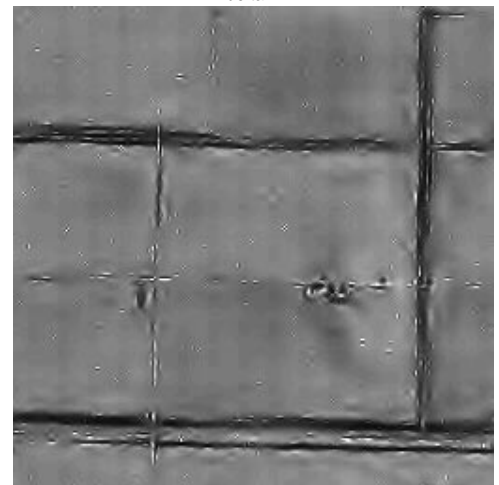
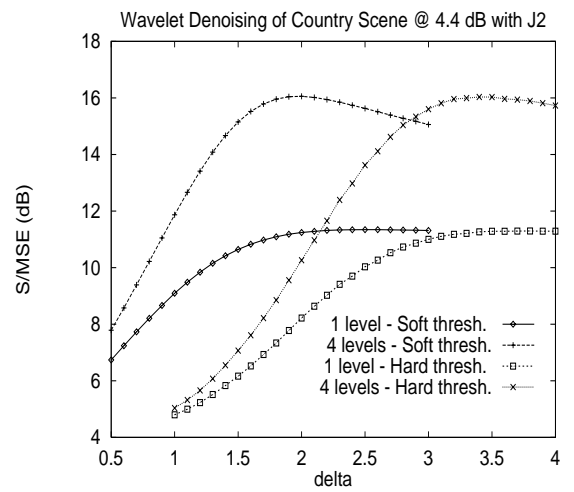
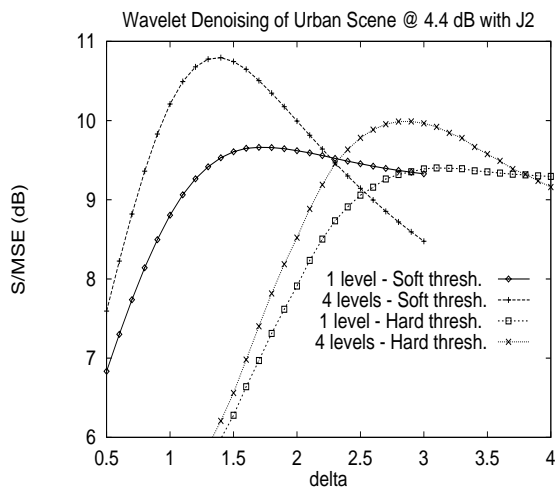


Figure 7: Wavelet denoising of the urban and country scenes @ 4.4 dB with J2

## 4 Discussion and Conclusion

We have presented a numerical study of a complex WCS speckle filter that specifically addresses the change (1) in the regularity and type of the wavelet (orthogonal versus bi-orthogonal) and (2) in the wavelet coefficient thresholding type (soft- versus hard-thresholding). We also gave measures of the variation of the S/MSE ratio over a wide range of filter parameters in order to get information on the optimal application range of the filter in practical situations. Tests were performed on simulated imagery with a multiplicative Log-Normal noise. The S/MSE ratio was measured after averaging the filtered images over 16 diagonal shifts in order to approximate a shift-invariant DWT.

Our experiments show that the optimal threshold level depends on the spectral content of the image. High spectral content tends to over-estimate the noise standard deviation estimation performed at the finest level of the DWT. As a result, a lower threshold parameter  $\delta$  is required to get the optimal S/MSE. The standard WCS theory predicts a threshold that depends on the number of signal samples only [7].

The experiments also show that the soft-thresholding scheme is always the better choice (in terms of S/MSE) especially for images with high spectral content. With a different data set (i.e. 1D signals with additive Gaussian noise), other authors have reported better results for a hard-thresholding scheme when applied in combination with a shift-invariant DWT [10, 11]. We believe the difference is a consequence of the noise characteristics. Further tests are needed to clarify this point.

Finally, as theoretically developed in [9], denoising with bi-orthogonal wavelets requires a larger threshold than for orthogonal ones. Also, some bi-orthogonal wavelets are quite robust to the orthogonality requirement of the WCS scheme. In particular, first order spline-based wavelets bi22 and bi24 performed almost as well as J2 wavelets which is clearly the best choice of all. This indicates that a WCS scheme that is properly adapted to bi-orthogonal wavelets, i.e. that incorporates correlations between wavelet coefficients, could also yield a performant filter [9]. We are currently implementing such a scheme and test results will be reported soon.

## References

[1] L. Gagnon, F. D. Smaili, "Speckle Noise Reduction of Airborne SAR Images with Symmetric Daubechies Wavelets", SPIE Proc. #2759, pp. 1424, 1996

[2] L. Gagnon, A. Jouan, "Speckle Filtering of SAR Images - A Comparative Study Between Complex-Wavelet-Based and Stan-

dard Filters", SPIE Proc. #3169, pp. 80-91, 1997

[3] D. R. Wehner, "High-Resolution Radar", 2nd Edition (Artech House, Boston, 1994)

[4] H. C. Shyu, Y. S. Sun, W. H. Shen, "The Analysis of Scan-to-Scan Integration Techniques for Sea Clutter", IEEE Proc. Nat. Radar Conf., pp. 228-233, 1994

[5] V. S. Frost, J. A. Stiles, K. S. Shanmugan, J. C. Holtzman, "A Model for Radar Images and Its Application to Adaptive Digital Filtering of Multiplicative Noise", IEEE Trans. PAMI, Vol. PAMI-4, pp. 157-166, 1982

[6] A. Lopes, E. Nezry, R. Touzi, H. Laur, "Structure Detection and Statistical Adaptive Speckle Filtering in SAR Images", Int. J. Remote Sensing, Vol. 14, pp. 1735-1758, 1993

[7] D. L. Donoho, "Denoising by Soft-Thresholding", IEEE Transactions on Information Theory 41, 613-627, 1995

[8] J. M. Lina, M. Mayrand, "Complex Daubechies Wavelets", App. Comp. Harmonic Anal., Vol. 2, pp. 219-229, 1995

[9] K. Berkner, R. O. Wells Jr, "A Correlation-Dependent Model for Denoising via Nonorthogonal Wavelet Transforms", Computational Mathematics Laboratory, Rice Univ., Technical Reports 98-07

[10] R. R. Coifman, D. L. Donoho, "Translation invariant denoising", in Wavelets and Statistics, (Springer-Verlag, 1995)

[11] M. Lang, H. Guo, J. E. Odegard, C. S. Burrus, R. O. Wells Jr., "Noise Reduction Using an Undecimated Discrete Wavelet Transform", IEEE Signal Processing Letters 3, 10-12, 1996